We are IntechOpen, the world's leading publisher of Open Access books Built by scientists, for scientists

4,800
Open access books available

122,000
International authors and editors

135M
Downloads

Our authors are among the

154
Countries delivered to

TOP 1%
most cited scientists

12.2%
Contributors from top 500 universities

CLARIVATE ANALYTICS BOOK CITATION INDEX INDEXED

WEB OF SCIENCE™

Selection of our books indexed in the Book Citation Index in Web of Science™ Core Collection (BKCI)

Interested in publishing with us?
Contact book.department@intechopen.com

Numbers displayed above are based on latest data collected.
For more information visit www.intechopen.com

Chapter 4

Forming of Sandwich Sheets Considering Changing Damping Properties

Bernd Engel and Johannes Buhl

Additional information is available at the end of the chapter

http://dx.doi.org/10.5772/50565

1. Introduction

1.1. Sandwich sheets

For many applications there are claims concerning the metal sheet, which cannot be reached with a single sheet. Composite materials, which can be classified in fiber-composites, sandwich materials and particle-composites are increasing year by year [1]. Sandwich respectively laminates with various thicknesses and materials of the different layers offer highly useful properties. As seen in Figure 1 every material has different mechanical, acoustical, tribological, thermal, electrical, chemical as well as environmental and technological properties.

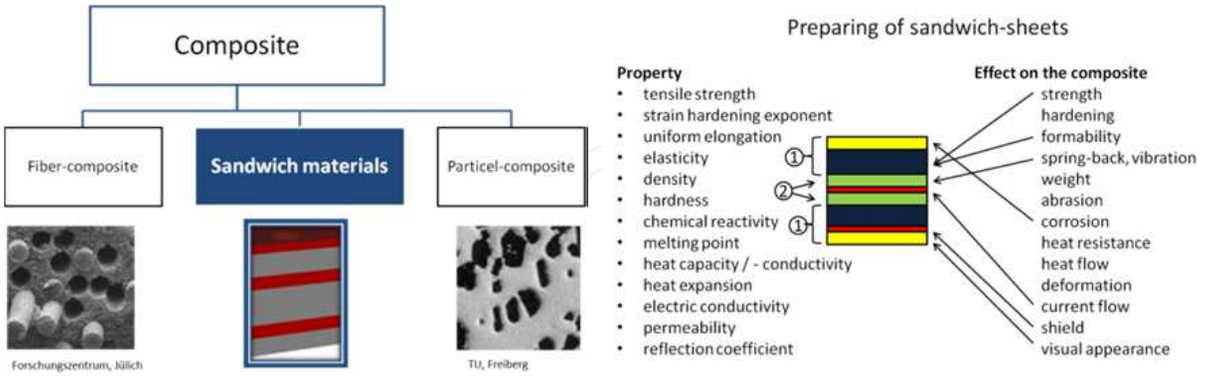

Figure 1. Classification of composites; preparing of sandwich sheets

Figure 1 illustrates an example of a fictive constellation of a composite. The price of the raw material itself has to be lower than the price of stainless steel. The nearly symmetrical sandwich should be resistant against corrosion and appear like stainless steel. For application in the automotive industry, it should be highly formable and reduce vibrations.

So the thin outer sheets are chosen of 1.4301, the supporting layer of DC06 and the vibration damping layer of a viscoelastic adhesive. At first, the metal layers of both sides are cladded 1. In step no. 2 they are bonded with a very thin adhesive layer (see chapter 5.4). To achieve advantages concerning the forming process (see chapter 4.1), a metal interlayer is included.

1.2. Failure-modes of sandwich sheets

Sheets with vibration damping qualities can be made of steel sheets enclosing a viscoelastic plasticcorelayer (see Figure 17). [2] The vibration energy of the oscillating coversheet is converted into heat.[3] [4] For automotive lightweight constructions, sandwich sheets with a noise-absorbent behavior are highly useful in the engine bay. [5]

Parts of sandwich sheets with viscoelastic layers excel with a higher security against cracking. [6]

Due to the relocatability of the outer and the inner sheet, leakage of e.g. an oil pan in contact with the subsoil or in case of a crash is unlikely for this sandwich in contrast to a comparable single layer sheet. The cover-sheets remain undamaged, but the bond can fail during forming. Under load, during and after the forming process special effects and failures occur. [7]

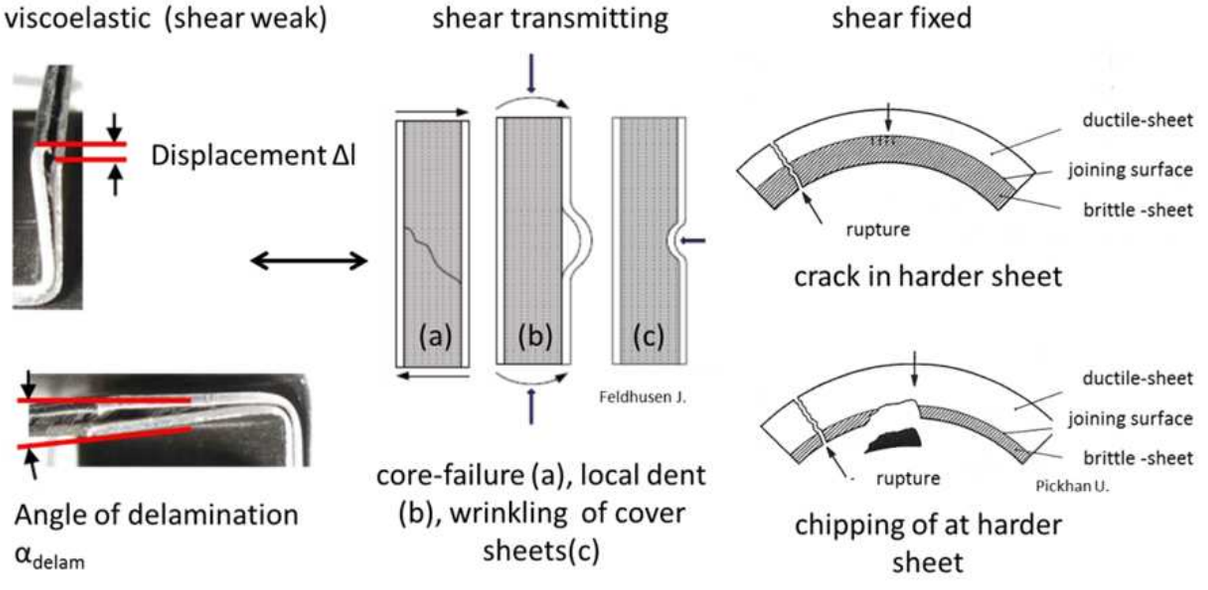

Figure 2. Failure modes of during forming of sandwich sheets (viscoelastic, shear transmitting and shear fixed)

Mainly displacement and delamination of the cover sheets occur as failure modes (see Figure 2). Wrinkling at the inside surface is detected especially by vibration-damping composite sheets with long non-deformed legs and small thickness of the inner layer. Plastics and adhesives creep under load. [8] Because of the residual stresses in the cover sheets or due to temperature influences, the composite delaminates often after hours or days, respectively.[9] To decay noises effectively, the viscoelastic interlayer has to be as thin as possible (chapter 5). In contrast to this, lightweight sandwich sheets achieve great

stiffnesses with thick synthetic cores. [10] As well as by shear weak connection, the cover layer of shear transmitting sandwiches usually does not crack. Now, additive failures like core-failure, local dents and wrinkling of cover sheets limit the forming capabilities. [11] Typically, laminates which are jointed shear fixed crack on the brittle side. [12]

1.3. Classification of sandwich sheets

The joining process of several layers has a great influence of the formability and the damping behavior of the sandwich. Layers can be connected viscoelasticly by using an adhesive film. The cover sheets are allowed to slide on each other. For that displacement only a negligible shear force is necessary. This viscoelastic bond is weak. Shear transmitting bond lines like 1 or 2 component-adhesives are ductile. Parameters of the roll bonding process and surface treatments are shown in [10]. Layers which are connected shear fixed (cladded) can´t slide on each other. [15] In a forming process the sheet behaves like a single sheet, but after forming, astonishing effects due to different Young's moduli and hardness occur.

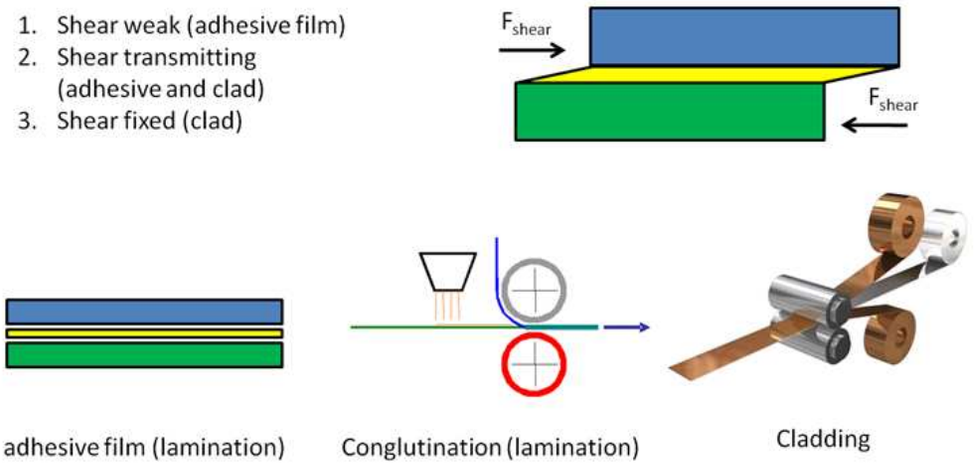

Figure 3. Classification of joining with respect to transmitting shear force

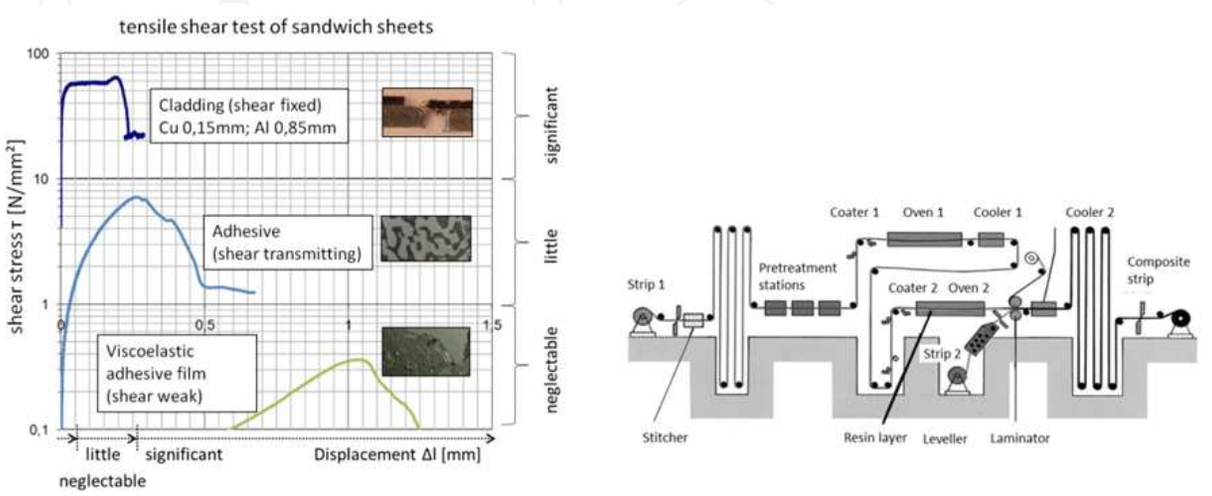

Figure 4. Tensile shear test of sandwich sheets; Strip production line similar to [3]

This classification is confirmed with tensile shear tests. As seen in Figure 4 the link surface of cladded sheets remains undamaged. This example shows a layer of copper (thickness $t_{co} = 0{,}15\,mm$) and aluminum (thickness $t_{al} = 0{,}85\,mm$). Under a shear stress of approximately $\tau = 60\ \mathrm{N/mm^2}$, the layer of aluminum cracks under $\alpha = 45°$ degree. Cladded sandwich sheets are produced for thermal protection shields, pipe clamps, and safety components in automotive section, microwaves, cutting punches, heat exchanger and bipolar collector plate. [13],[14],[15]

Little shear stress can be transmitted with an adhesive layer which shows tow fracture appearances, the adhesive and cohesive crack. This type of sandwich sheets is often laminated as seen in Figure 4. A strip production line comprises a decoiler for the strip 1, an alkaline degreasing and chemical pretreatment of strip 1, a coater of strip 1 with the resin layer (applied on coater 2), a continuous curing oven 2, and a decoiler for strip 2. Then, it follows the laminator which rolls strip 1 and 2 into the composite strip material. After laminating the sandwich sheet is cooled in station 2 and recoiled. [5] Further this shear transmitting sandwich sheets are considered.

When viscoelastic interlayers, performed as an adhesive film, reach their maximal displacement, the adhesive detaches of the cover sheets.

2. Experimental tests and their simulation

Material properties will be determined by experimental tests. The connection should be classified with tensile shear tests. All tests are carried out at room temperature. For vibrations damping sandwich sheets, the parameters of different approaches will be computed. The advantages of the different approaches will be discussed.

Main experimental tests to get information of the forming behavior will be described and illustrated with examples.

2.1. Uniaxial tensile test

The relation between stress and strain for uniaxial tension is determined with tension tests. [16] The tests are carried out under an ambient air temperature of $t_{air} = 22$ °C with a tension velocity of $v = 0{,}05$ mm/s. The yield strength ($R_{p0,2}$), tensile strength (R_m), and uniform elongation (φ_{gl}) of cover sheets were read out. DC04, DC06, 1.4301 and 1.4640 are chosen for the cover-sheet material. Three tensile tests carried out under the same conditions are shown in Figure 5 (cover sheet material: DC06).

For further analytical calculations of the strain-distribution, the bending-moment and the shear-force, the plastic behavior of the sheet material is described linearly with the gradient m, see equation (1).

$$k_{f\_lin} = R_{p0,2} + \varphi m \qquad m = \frac{(1+\varepsilon_{gl})R_m - R_{p0,2}}{\varepsilon_{gl} - \frac{R_{p0,2}}{E}} \tag{1}$$

Out of a composition of common different material descriptions (Table 1), the stress-strain relation for numerical calculations is described according to Swift/Krupkowski k_{f_Swift} [17]. This three-parameter model describes an exponential function. The parameters can be found by using numerical optimizations. Furthermore, the parameters are determined using the instability-criterion, the strain hardening coefficient n, uniform elongation A_g and so on according [18]:

$$k_{f\_Swift} = b(c + \ln(1+\epsilon))^d \qquad n = \varphi_v \approx \ln(1+A_g) \tag{2}$$

$$c = \sqrt[n]{\frac{R_{p0,2}}{R_m}}\frac{n}{e} \qquad d = (c+n) \qquad b = R_m * \frac{e^n}{d^d} \tag{3}$$

So, the following Table 1 can be established.

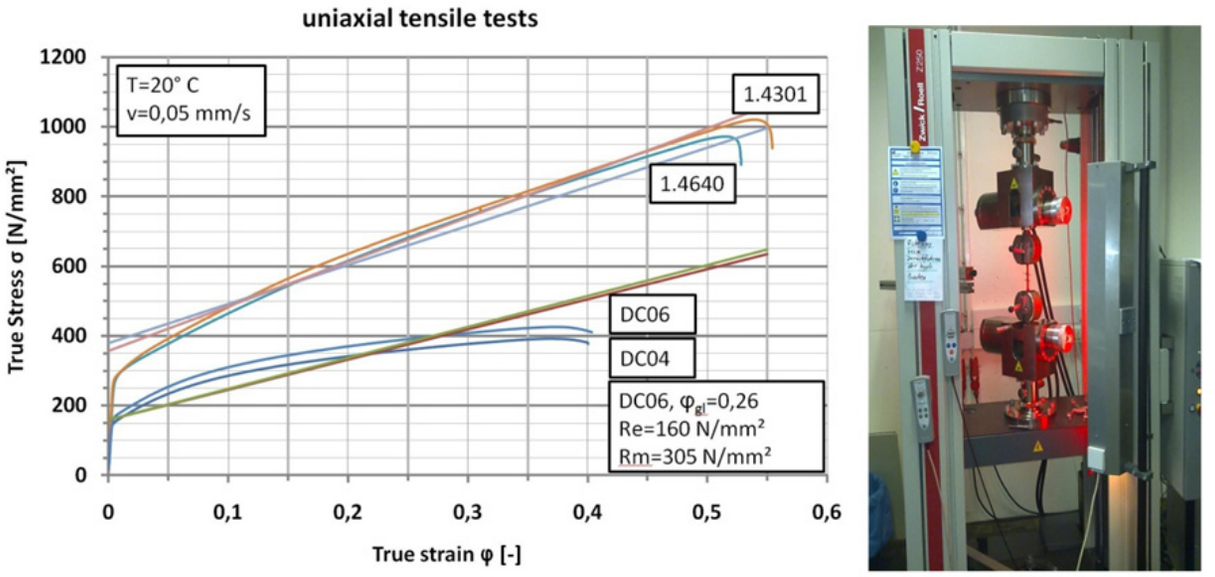

Figure 5. Uniaxial tensile tests of the metal sheet layer [6], Universal testing machine

	DC 04	1.4301	1.4640	DC06
d	0,284	0,443	0,370	0,236
c	0,061	0,043	0,029	0,005
b	545	1337	1268	540
n	0,2231	0,4007	0,3414	0,2311

Reihle/Nadai:	$k_f = c_1 * {\varphi_v}^n$	(4)
Swift/Kurp.:	$k_f = c_1(c_2 + \varphi_v)^n$	(5)
Gosh:	$k_f = c_1(c_2 * \varphi_v)^n - c_3$	(6)
Voce:	$k_f = c_2 - (c_2 - c_1)e^{(-c_3\varphi_v)}$	(7)
Hocket-Sherby:	$k_f = c_2 - (c_2 - c_1)e^{(-c_3 * {\varphi_v}^n)}$	(8)
Extrapolation Rein-Alu :	$k_f = c_1 * {\varphi_v}^n * e^{\left(\frac{-c_3}{\varphi_v}\right)}$	(9)

Table 1. Material parameters for Swift/Krupkowski, composition of common material models

2.2. Tensile shear test

During the forming process the cover layers of the sandwich slide on each other. By shifting the cover plates the adhesive layer is sheared. Tensile shear tests provide the stress-displacement behavior of the adhesive for a constant shear rate at room temperature. They can be transferred directly to the forming process [6]. Different adhesives applied in liquid state were investigated. In addition, sandwich sheets of Bondal® [5] CB (Car Body) from ThyssenKrupp are considered. As seen in Figure 6, the specimens were prepared according to DIN 53 281 [19] respectively [20] but also [21]. The thicknesses of the cover sheets ($s = 0{,}75\,mm$) and of the adhesive layer ($s_{ad} = 0{,}05\,mm$) are given by the composite material. In Figure 6 three tensile shear tests of sandwich sheets with different testing velocities are shown. The shear stress is calculated from the initial overlapping length $L_{ü}$ and the gauged force F.

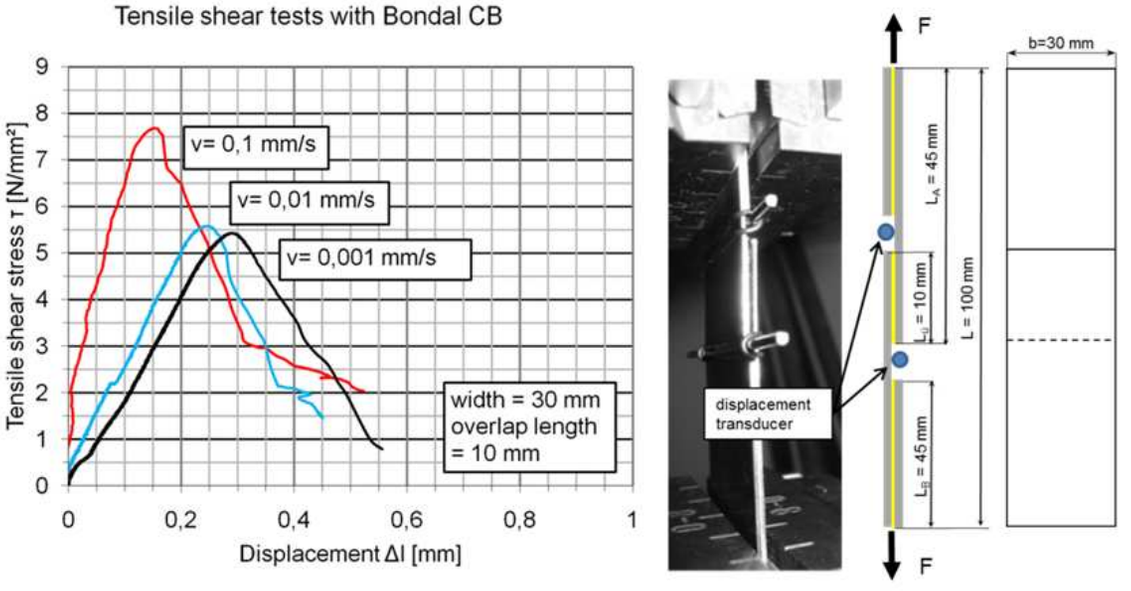

Figure 6. Tensile shear test with Bondal CB (cover sheets of DC06), specimen geometry

The adhesive layer fails by reaching the maximum force. For composites with a shear transmitting adhesive a shear stroke of $\overline{\Delta l}_{max} \approx 0{,}22$ mm was determined at a maximum shear stress of $\overline{\tau}_{max} \approx 5{,}5\ \frac{N}{mm^2}$ (see Figure 6). These values were computed by arithmetic mean. With higher velocity, the shear stress increase, but the tolerable displacement drops. The specific stiffness of the adhesive ($\frac{E}{Knn} = \frac{\tau_{max}}{\Delta s}$), a measurement to describe the increase of the shear stress, rises.

Delamination and displacement of laminated metal sheet can be analyzed by using finite elements. In Figure 7 the experimental and numerical tensile shear tests of the adhesive film are shown. In literature, several investigations determined the stress distribution depending on the overlapping lengths [8]. As the experimental tensile shear test, the force F and displacement Δl are gauged with numerical calculations. The shear stress is determined by

the force, as well as by the initial overlapping length. There are different modes of delamination. G. Alfano and M. A. Crisfield e.g. established an interaction model "mixed-mode" which summarizes many fracture criteria proposed in literature. [22] To describe the elasticity of the adhesive, the traction/relative displacement law is used. The damage law with nominal stress of the normal mode and the both other directions is chosen. Numerical results of the uniaxial tensile shear tests fit to the experiments. Special attention for forming sandwich sheets is laid on the failure of the adhesive bond. As seen in Figure 7 the elastic and damage behavior is calculated exactly, but the maximal shear force and displacement depart up to 9 %.

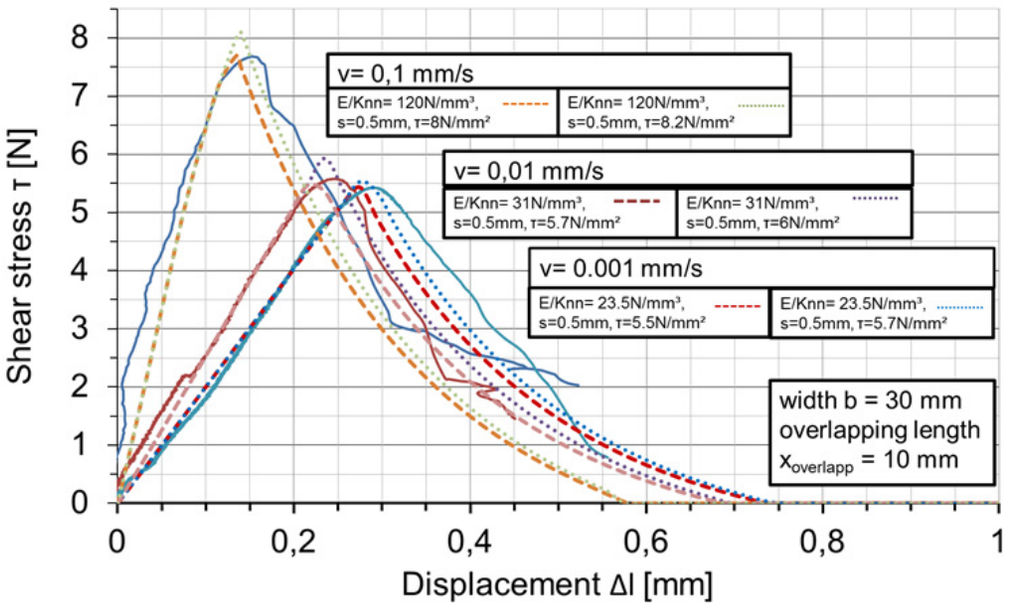

Figure 7. Numerical calculation of tensile shear tests

3. Forming tests: Die-bending

To predict the suitability of vibration-damping sandwich sheets for forming, material properties and interactions are calibrated with the simulation of the die-bending tests. V-die bending with different temperatures are considered in [23] and of velocity in [24]. Therefore specimens with a special grid on the surface of edge were prepared.

Optimized adhesive parameters for numerical calculation are applied on the shear test (see Figure 7). With bilinear, quadrilateral elements the material is performed. Reduced integration plane stress space with hourglass control (CPS4R) is used. Hard pressure-overclosure behavior is approximated with the penalty method. The penetration distance is proportional to the contact force. Contact is implemented frictionless to assume that surfaces in contact slide freely and isotropic with a friction-coefficient of $\mu_{werk} = 0{,}1$.

In Figure 8 the v-die bending process of a symmetrical sandwich with a length of 2L is considered. The stress, strain and displacement of both cover sheets out of DC06 with a thickness of s = 0,7 mm are determinant for two zones, the bending area and the adjacent

area. By the punch radius r and the bending angle α, the bending area is defined. In contrary to homogeneous sheets, the adjacent area of the bending area shows a significant stress distribution. This leads to a plasticization of the primarily adjacent area. The residual stress also leads to delamination even after weeks or even under influence of temperature.

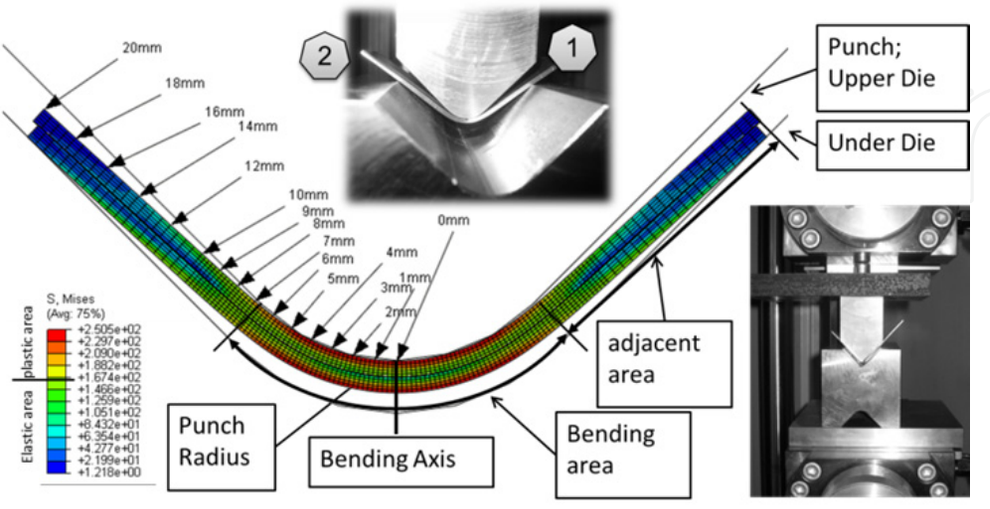

Figure 8. Pilot project: Experiment v-die bending, v-die bending with cover sheet material DC06

The adhesive layer transmits shear-force of the bending area into the adjacent area. For distances t = [1, 2, 3…] mm from the bending axis the displacement is measured in the simulation and experimental tests. Accurate preparing of the specimens for die bending has a great influence on applicability of the results. After polishing the surfaces of the edges, a micro grid is scribed with a depth of t_{dia} = 3 µm. At the inflection line of the chamfer with the width b_{dia} = 5 µm the light reflects and a sharp line can be seen. For scribing, a diamond with a point angle of α_{dia} = 130° is used. Figure 9 shows calculated and experimental displacements of cover sheets after bending. With the influence of manufacturing, the enlarged displacements of experimental tests are explained. The simulation-model is verified.

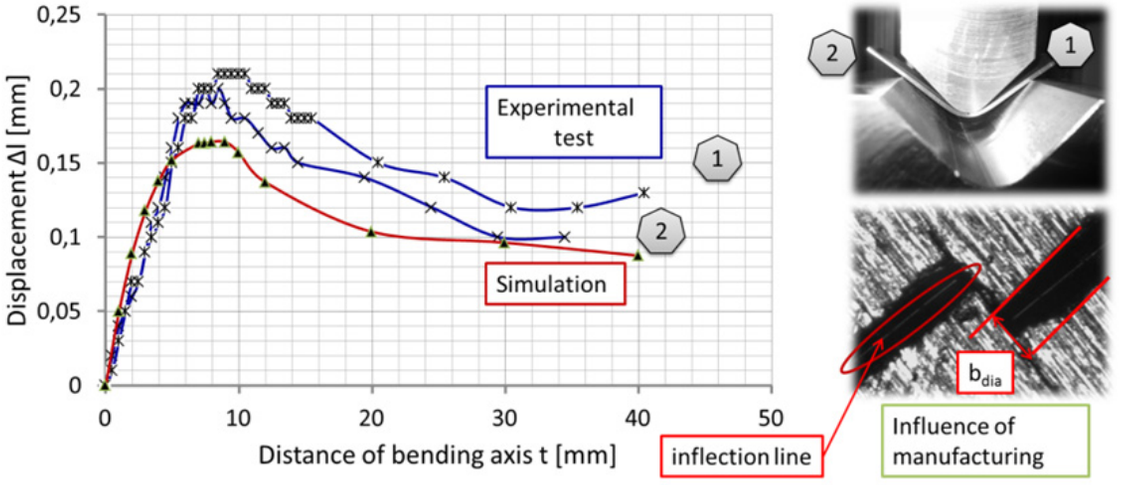

Figure 9. Pilot project v-die bending: calculated and experimental displacement of cover sheets, material DC06 (b)

Normally, only the edges of a formed part can be seen. Thus, the displacement of the sheets in the bending area is not detectable. At first the displacement of the edges depends on the side length L = [40, 35, 30, and 25] mm, see Figure 10. As expected, increasing side length causes decreasing displacement.

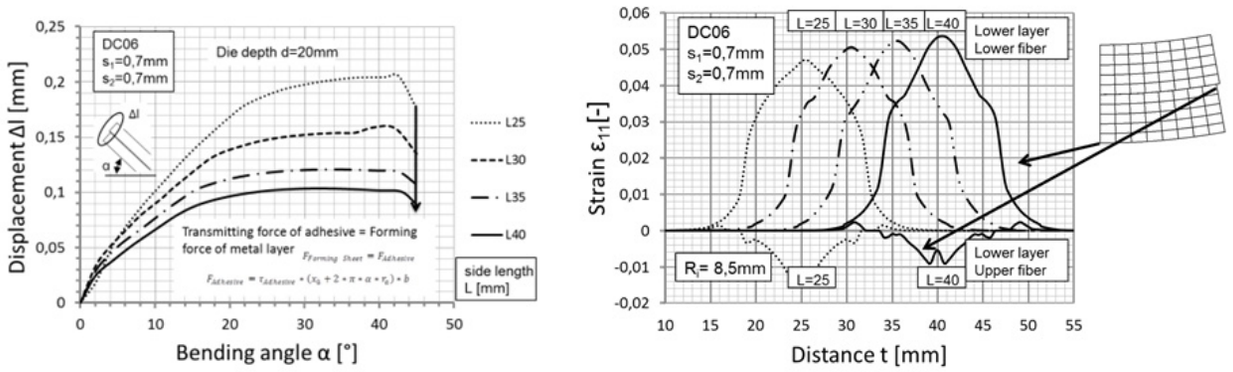

Figure 10. Numerical results of die-bending; displacement Δl over bending radius α for variation of side length L (a), elongation of the external fiber of the both layers with bending axis at distance t = 40 mm (b)

Also the strain of the upper and under fiber of the under layer in bending direction is shown. With larger side lengths the strain increases and a special peek of strain occurs in the bending center. The neutral axis of the lower cover-layer moved depending on the side length in direction to the upper fiber. In the upper layer, the neutral axis moved to the midst of the sandwich sheet, too. Further strain distributions of other fibers, the influence of friction and several displacements dependent on the distance from the bending axis in the bending and adjacent area are shown in [25]. Also the influence of adhesive in contrast to tow single sheets, which slide frictionless on each other, can be seen. So a cutback of the edge displacement from Δl = 0,37 mm to 0,09 mm (L = 40 mm) is achieved with a viscoelastic adhesive. From this it follows that the shear transmitting interlayer doesn't fail at the edges. But at the beginning of the adjacent area, the displacement crosses Δl = 0,15 mm by already a bending angle α = 30°.

Even sandwich sheets with large side lengths of for example L = 40 mm can gain an inner failures during forming. Simulations with adjusted layer-thickness are shown in chapter 6.

4. Plastomechanical preliminary design

Correct use of simulation tools demands experiences in element types, material laws, contact properties, solver and integration step characteristics to evaluate numerical results. Moreover the calculation requires high calculation time and performance. [26]

To reduce the calculation time a plastomechanical preliminary design is established (see Figure 11). Several numerical calculations describe the bending behavior of three-layer sandwich sheets with viscoelastic interlayers. Numerical investigations are made by M.

Weiss for the elastic [27] and TAKIGUCHI for the plastic [28] bending process of three layer sandwich plates.

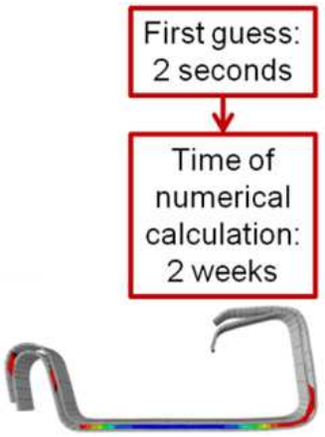

Figure 11. Aim of plastomechanical preliminary design

Proposals to calculate the reached length of shear fixed sandwich sheets are established of Hudayari [29]. With the following two methods "viscoelastic" and "shear transmitting", simple proposals for designing the thickness ratio of the metal layers and the required shear stress are made. Especially the "viscoelastic" description of the forming of sandwich sheets is qualified for basic statements.

4.1. Three-layer sandwich with viscoelastic interlayer

Sandwich sheets with an adhesive film show displacements and delamination very clearly. At a specific displacement $\overline{\Delta l}_{max}$ the interlayer fails. When the adhesive delaminates from the sheets, the cohesive force is small and can be neglected. Therefore, the cohesive force is not include in this "viscoelastic model"; neither to determine displacement, nor of the angle of delamination α_{delam}.

As explained in [6], the Euler–Bernoulli beam theory [30] is used. The neutral axis remains in the middle of each layer. With following geometric relations, the technical strain ε can be determined in dependency of the radius of the neutral axis R_n and the control variable y:

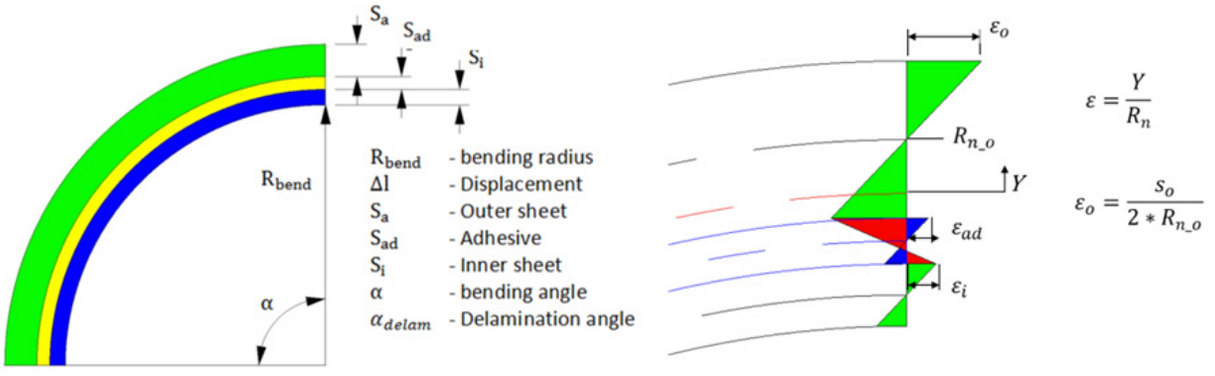

Figure 12. Geometrical description of the bending process [6] and strain distribution over thickness

$$\Delta l = \alpha * 0.5 * (s_a + s_i) \tag{10}$$

Independent of the bending radius R_{bend}, the geometric displacement Δl is determined with the bending angle α and the sum of layer-thicknesses S_a and S_i (equation (10)). This approach fits quite well [6]. Since the adhesive layer is thin, it can be neglected. Over the thickness of the cover-layers, as well as over the bending angle, a linear strain distribution is assumed. The spring-back angle α_{sb} is calculated from the integration of the back-curvature under usage of a linear-plastic material model according [31]:

$$\alpha_r = \int_{x=0}^{x=r\alpha} \frac{2*\sigma_{ael}}{E*s} dx = \frac{2*\sigma_{ael}}{E*s} R_n \alpha \tag{11}$$

With σ_{a_el} for the stress which relaxes during spring back:

$$\sigma_{a\_el} = \frac{6{R_n}^2}{s^2}\left(\frac{2}{3}\left(\frac{R_{p0,2}}{E}\right)^3\left(E + \frac{m}{2}\right) - \left(\frac{R_{p0,2}}{E}\right)^2 R_{p0,2}\right) + \frac{s}{2r}m + 1{,}5(R_{p0,2} - \frac{R_{p0,2}}{E}m) \tag{12}$$

Neglecting small terms, the spring-back angles α_{sb} are determined for each layer:

$$\alpha_{sb} \approx 3\frac{R_{p0,2}}{E} * \frac{R_n}{s} * \alpha \tag{13}$$

The angle of delamination α_d from the difference of the two spring-back angles is calculated:

$$\alpha_d = \alpha_{sb\_a} - \alpha_{sb_i} \tag{14}$$

For the same materials of both cover layers the delamination α_d is established relating to the inner radius of the sandwich sheet R_{bend}:

$$\alpha_{d\_mat} \approx 3\alpha\frac{R_{p0,2}}{E}\left(\frac{s_i R_{bend} + s_i s_i + s_{ad} s_i - s_a R_{bend})}{s_i * s_a}\right) \tag{15}$$

And for the same thicknesses $S = S_i = S_a$ of the cover sheets:

$$\alpha_{d\_th} \approx \frac{3\alpha}{s}\left(\frac{R_{p0,2\_a}}{E_a} * (R_{bend} + s_{ad} + 1{,}5 * s) - \frac{R_{p0,2_i}}{E_i}(R_{bend} + 0{,}5 * s)\right) \tag{16}$$

Standardly, sandwich sheets are produced and as a matter of fact have the same cover-materials and thicknesses. S_{ad} is the thickness of the adhesive:

$$\alpha_{d\_mat\_th} \approx 3\alpha\frac{R_{p0,2}}{E}\left(\frac{s^2 + s_{ad}s)}{s^2}\right) \tag{17}$$

Regarding to these calculations the following options to prevent the tendency of delamination were identified by [6]:

- The softer material should be chosen as the inner layer. But the inner layer has to bear the forming forces.
- Angle increases by reducing the thickness. If the thinner layer forms the inner curve, the inner layer springs against the outer. [6] shows, that no delamination occurs for a specific thickness ratio.
- Overbending is another method to avoid delamination. So elastic stress, which results from the different angle, leads to a compressive stress at the contact surfaces after bending back.

- The delamination can be prevented by pre-bending with a smaller radius. With the expansion of the radius in the forming process, the different angle of the cover sheets is used.

4.2. Sandwich sheets with shear transmitting interlayer

As described by the tensile shear tests in chapter 2.2, the metal layers can slide on each other under shear force. The adhesive layer has been considered as viscoelastic. Now, sandwich sheets with shear transmitting interlayers are considered. The neutral axis of the cover lower layer moved depended on the side length (chapter 3) and the shear stress τ_{max} of the adhesive. In the upper layer, the neutral axis moved to the midst of the sandwich sheet, too.

So the shear force of the adhesive, which superposes the bending moment M_b with the force $F_ü$, constitutes the shifting of the axis. The shifting of the neutral axis is expressed by the k-factor (Figure 13). The compressive strain and elongation of the cover sheets changes. Part (b) of Figure 13 shows the outer cover sheet of a symmetrical shear-fixed sandwich. Strain modes of a sandwich layer, which transmits no $F_ü = 0$, $k_i = k_a = 0$ (c), tension (a, b) or even compression forces (d, e), are shown.

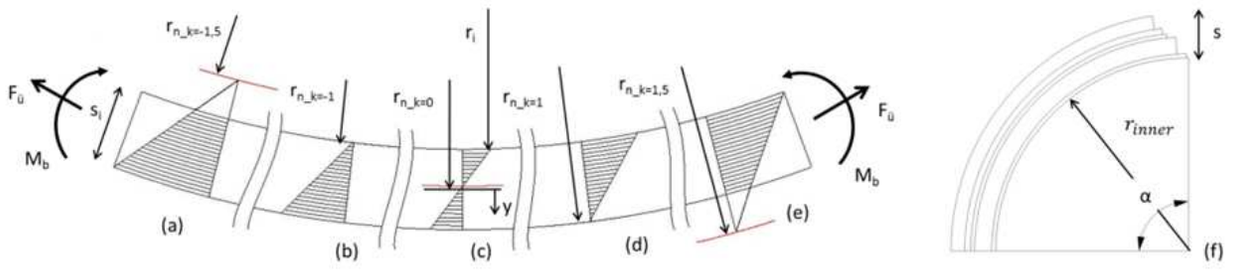

Figure 13. Principle of k-factor for each layer (a-e), geometric of a sandwich with different layer-thicknesses (f) and a layer under a bending moment (g)

The strain distribution of sandwiches with i metal layers, which may have different thicknesses s_i, can be described by the k-factor. For each metal layer with the thickness s_i, the neutral axis R_n i is computed dependent on the thickness of the sandwich s:

$$r_{m,i,n} = r_{inner,i,n} + \left(1 + k_{i,n}\right) \cdot \frac{s_i}{2} \tag{18}$$

The bending radius r_{inner} refers to the inside of the sandwich. Considering this, the true bending moment $M_{B,i,n}$ is:

$$M_{B,i,n} = \underbrace{\int_0^{\frac{s_i}{2}\cdot\left(1-k_{i,n}\right)} \sigma_{plast,i,n} \cdot b \cdot y \cdot dy}_{tension} + \underbrace{\int_{-\frac{s_i}{2}\cdot\left(1+k_{i,n}\right)}^{0} \sigma_{elast-plast,i,n} \cdot b \cdot y \cdot dy}_{compression} \tag{19}$$

Integration of the bending moment leads to dependency of the k-factor:

$$M_{B,i,n} = A_i \left(A_{0,i,n} + A_{1,i,n} \cdot k_{i,n} + A_{2,i} \cdot k_{i,n}^2 \right) + m_i \cdot I_{Z,i} \frac{1 + 3 \cdot k_{i,n}^2}{r_{m,i,n}} \tag{20}$$

$$\begin{aligned} A_i &= R_{p0.2,i} \cdot \left(1 - \frac{m_i}{E_i} \right) \cdot b \\ A_{0,i,n} &= \frac{s_i^2}{4} - \frac{1}{3} \cdot \left(\frac{R_{p0.2,i}}{E_i} \right)^2 \cdot \left(r_{innen,i,n} + \frac{s_i}{2} \right)^2 \\ A_{1,i,n} &= -\frac{1}{3} \cdot \left(\frac{R_{p0.2,i}}{E_i} \right)^2 \cdot \left(r_{innen,i,n} + \frac{s_i}{2} \right) \cdot s_i \\ A_{2,i} &= \frac{s_i^2}{4} - \frac{1}{3} \cdot \left(\frac{R_{p0.2,i}}{E_i} \cdot \frac{s_i}{2} \right)^2 \end{aligned} \tag{21}$$

With the moment of inertia $I_{z,i}$ of a rectangular cross-section:

$$I_{z,i} = \frac{b \cdot s_i^3}{12} \tag{22}$$

Substituting the bending moment under load M_B with the elastic bending moment $M_{B\text{-}el}$, the radius of curvature K can be determined for the unloaded case.

$$M_{B-el,i,n} = \frac{b}{r_{R,i,n}} \cdot E_i \cdot \int_{-\frac{s_i}{2}\left(1+k_{i,n}\right)}^{\frac{s_i}{2}\left(1-k_{i,n}\right)} y^2 \cdot dy = \frac{1}{r_{R,i,n}} \cdot E_i \cdot I_{z,i} \cdot \left(1 + 3 \cdot k_{i,n}^2 \right) \tag{23}$$

$$\kappa_{R,i,n} = \frac{M_{B,i,n}}{E_i \cdot I_{z,i} \cdot \left(1 + 3 \cdot k_{i,n}^2 \right)} \tag{24}$$

So, the remaining radius α_{bl} is calculated:

$$\alpha_{bl,i,n} = \int_0^{r_{m,i,n} \cdot \alpha_n} \kappa_{bl,i,n} \cdot d\alpha = \left(1 - \kappa_{R,i,n} \cdot r_{m,i,n} \right) \cdot \alpha_n \tag{25}$$

$$\alpha_{bl} = 1 - B \frac{\left(B_0 + B_1 \cdot k + B_2 \cdot k^2 + B_3 \cdot k^3 \right)}{\left(1 + 3 \cdot k^2 \right)} - \frac{m}{E} \tag{26}$$

$$B = \frac{R_{p0.2}}{E \cdot I_Z} \cdot \left(1 - \frac{m}{E}\right) \cdot b$$

$$B_0 = \frac{s^2}{4} \cdot \left(r_{innen} + \frac{s}{2}\right) - \frac{1}{3} \cdot \frac{R_{p0.2}^2}{E^2} \cdot \left(r_{innen} + \frac{s}{2}\right)^3$$

$$B_1 = \frac{s^3}{8} - \frac{1}{2} \cdot \frac{R_{p0.2}^2}{E^2} \cdot \left(r_{innen} + \frac{s}{2}\right)^2 \cdot s \tag{27}$$

$$B_2 = \left(1 - \frac{1}{3} \cdot \frac{R_{p0.2}^2}{E^2}\right) \cdot \frac{s^2}{4} \cdot \left(r_{innen} + \frac{s}{2}\right)$$

$$B_3 = \left(1 - \frac{1}{3} \cdot \frac{R_{p0.2}^2}{E^2}\right) \cdot \frac{s^3}{8}$$

$$\Delta l_{j,n} = \Delta l_{j,n-1} + \left(\alpha_{bl,i,n} - \alpha_{bl,i-1,n}\right) \cdot r_{m,n} - \left(1 + k_i\right) \cdot \frac{s_i}{2} \cdot \alpha_{bl,i,n} - \left(1 - k_{i-1}\right) \cdot \frac{s_{i-1}}{2} \cdot \alpha_{bl,i-1,n} \tag{28}$$

$$\Delta\alpha_{j,n} = \Delta\alpha_{j,n-1} + \left(\kappa_{R,i-1,n} - \kappa_{R,i,n}\right) \cdot r_{m,n} \cdot \alpha_n \tag{29}$$

In a multilayer sandwich sheet, the displacement Δl and the angle of delamination $\Delta\alpha$ between two layers can be calculated as shown in equation (28), (29). The determination of the k-factor and the following proposal list to avoid or minimize the failure modes at the edges are according to [25] :

- Keep the required overlapping length, respectively the side length
- Choose an adhesive depending on the shear force which is calculated
- Enlarge the number of metal layers
- Reduce the thicknesses of the outer layers
- Choose a material for outer layers with low yield strength
- Choose a small hardening coefficient

5. Acoustical calculations

5.1. The loss factor, a measurement for damping behavior of a material

The transmission of structure-borne noise depends highly on the behavior of a material. Through the temporal offset of the shear stress and strain, the vibration energy is converted into heat energy. [32], [33], [34]

A gauge of the internal damping of a material, the absorption capacity of vibrations, is the loss factor tan δ. With increasing loss factor the material behavior approaches a Newtonian fluid with viscosity. Even if the metal sheet is not damped by a polymeric coating or interlayer, the vibration of the sheet decays after a certain time. This effect is due to internal

friction of the solid. Compared to synthetic materials, steel converts a lower amount of vibration energy per oscillation into heat. The decay will take more time compared to a sandwich sheet. Using the poisson's ratio ν, the shear modulus is determined according to:

$$G = \frac{E}{2 \cdot (1+\vartheta)} \tag{30}$$

The loss factor is the ratio of storage modulus G' and loss modulus G'' [3]:

$$tan\ \delta = \frac{G'}{G''} \tag{31}$$

Complex shear modulus $G^* = G' + j \cdot G''$ with its amount $|G^*| = \sqrt{(G')^2 + (G'')^2}$ is highly dependent on temperature and amplitude. Often in a range of about 60 °C a constant value is assumed.

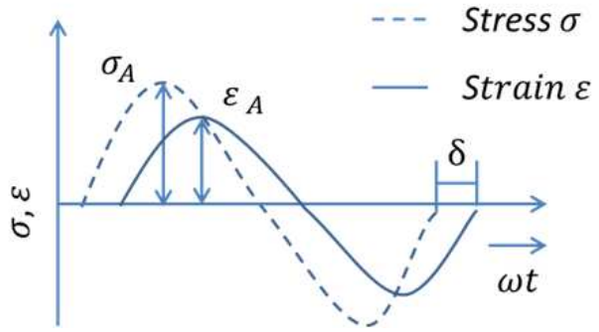

Figure 14. Offset between stress and strain over time

Material	loss factor tan δ
Steel	0,0006 – 0,0001
Aluminum	0,0001 – 0,001
Gray iron	0,01 – 0,02
Film of Bitumen	0,2 – 0,4
Damping mat	0,2 - 1

Material	tan δ [-]	E-Modulo [N/mm²]	T_{amb} [°C]	f [1/s]
Polyvinyl chloride	1,8	30	92	20
Polystyrene	2,0	300	140	2000
Polyisobutylene	2,0	6	20	3000
nitrile rubber	0,8	330	20	1000
hard rubber	1,0	200	60	40
Polyvinyl chloride with 30% plasticizer	0,8	20	50	100

Table 2. Loss factor tan δ for different materials under ambient temperature of T_{amb} = 20 °C [34] and Material properties according to [33]

Figure 15 shows the relation of the loss factor tan δ and the shear modulus, which leads to following equation:

$$G' = G \cdot cos(\delta) \tag{32}$$

Thus, the storage modulus G' can be detremined as:

$$G_2' = G \cdot cos(arctan(tan\delta_2)) \tag{33}$$

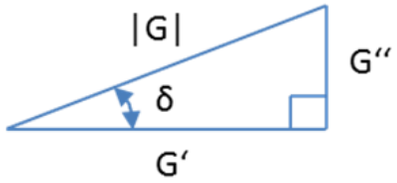

Calculated shear modulus G	
Young's modulus adhesive E [N/mm²]	6
Poisson's number ν [-]	0,49
Shear modulus G* [N/mm²]	2,013422819
Storage modulus G' [N/mm²]	0,900430058

Figure 15. Representation of a complex shear modulus |G*|, calculated values for the adhesive

5.2. Determination of decay behavior

In most calculations the damping effect is based on a linear combination of mass M and stiffness K. The sandwich sheet with viscoelastic damping subject following elasto mechanical system:

$$f_{(t)} = M\ddot{y} + C\dot{y} + Ky \tag{34}$$

M = mass matrix
K = stiffness matrix
C = damping matrix
y = displacement vector
$\dot{y}$ = velocity vector
$\ddot{y}$ = acceleration vector

Table 3. Parameters of the elasto-mechanical system: sandwich sheet with viscoelastic interlayer

The equation of motion in time includes damping by energy dispersion. Simplified, an initial displacement is assumed to generate the oscillation. This means that no force or impulse is considered in the calculation. This assumption simplifies the determination of the initial conditions to:

$$0 = \ddot{y} + \frac{c}{m}\dot{y} + \frac{k}{m}y \tag{35}$$

The terms $\frac{k}{m}$ and $\frac{c}{m}$ of the linear homogeneous equation can be transcribed with the relation of angular frequency of the undamped harmonic oscillation ω_0^2 and the damping ratio D to get the differential equation:

$$\omega_0^2 = \frac{k}{m} \tag{36}$$

$$D\omega_0 = \frac{c}{m} \tag{37}$$

$$0 = \ddot{y} + D\omega_0\dot{y} + \omega_0^2 y \tag{38}$$

The Euler representation with the function $sin(\omega_d \cdot t + \varphi_0)$ is used with the damped angular frequency ω_d. From experimental tests it is well known, that the decay based on displacement behaves $\hat{y}_0 \cdot e^{-\delta \cdot t}$ [35].

With $\hat{y}_0$, the value of the displacement at time $t = 0$:

$$y_{(t)} = \hat{y}_0 \cdot e^{-D\omega_0 \cdot t} \cdot sin(\omega_d \cdot t + \varphi_0) \tag{39}$$

With the following characteristics of:

Damping/ Decay constant:

$$\delta = tan\delta_{Sandwich} \cdot \pi \cdot f \tag{40}$$

Resonance quality:

$$Q = \frac{1}{tan\delta_{Sandwich}} \tag{41}$$

Damping ratio:

$$D' = \frac{tan\delta_{Sandwich}}{2} \tag{42}$$

The natural angular frequency of damped oscillation ω_d is calculated of angular frequency ω_0 and damping constant δ.

$$\omega_d = \sqrt{\omega_0^2 - \delta^2} \tag{43}$$

Due to the viscous damping, only the physically significant context $\omega_0^2 - \delta^2 > 0$ is considered further. With the dimensionless damping ratio D, the decay and input angular frequency can be compared:

$$D = \frac{\delta}{\omega_0} \tag{44}$$

5.3. Damping-behavior of a three layer sandwich

Ross, Kerwin and Unger (1959) [36] calculated with their approach "Damping Model" the damping behavior of a three-layer composite. Many modification has been made [37], [38], [39] with are summarized in [40]. Starting with the elastic bending moment M of the three-layer sheet, the shear forces and shear strains are calculated:

$$M = B\frac{\partial \Phi}{\partial \chi} = \sum_1^3 M_{ii} + \sum_1^3 F_i H_{io} \tag{45}$$

Where B is the flexural rigidity per unit width of the composite plate, M_{ii} the Moment of exerted by the forces on the i^{th} layer about its own neutral plane, F_i the net extensional force on the layer and H_{io} the distance from the center of the i^{th} layer to the neutral plane of the composite beam. [33] predicted the loss of "thick plates with a thin intermediate layer":

$$tan\delta_{Sandwich} = tan\delta_2 \cdot \frac{h \cdot g}{[[1+(1+i \cdot tan\delta_2) \cdot g]^2 + g \cdot h \cdot [1+g \cdot (1+tan\delta_2{}^2)]]} \quad (46)$$

With the "geometric parameter" 1/h, the distance between the neutral fiber of the sandwich structure and the coversheets is described.

$$\frac{1}{h} = \frac{B_1{}' + B_3{}'}{a^2} \cdot \left(\frac{1}{E_1 \cdot d_1} + \frac{1}{E_3 \cdot d_3}\right) \quad (47)$$

And a „shear-parameter“ g:

$$g = \frac{G_2'}{d_2 \cdot k^2} \cdot \left(\frac{1}{E_1 \cdot d_1} + \frac{1}{E_3 \cdot d_3}\right) \quad (48)$$

Parameter “a” is the distance of the neutral fibers of the cover plates:

$$a \approx d_2 + \frac{(d_1 + d_3)}{2} \quad (49)$$

And the number of wave k:

$$k = \left(\frac{\omega^2 \cdot m'}{B}\right)^{\frac{1}{4}} \quad (50)$$

With the mass per unit length m':

$$m' = \rho \cdot S \quad (51)$$

The cross-sectional area S:

$$S = lg(d_1 + d_2) \quad (52)$$

And with the specific total bending stiffness B':

$$B' = (B'_1 + B'_3) \cdot \left(1 + \frac{g \cdot h}{1+g \cdot (1+i \cdot tan\delta_2)}\right) \quad (53)$$

Wherein the specific bending stiffness B_i for a plane sheet layer can be calculated as:

$$B'_i = \frac{1}{12} \cdot E_i \cdot d_i^3 \quad (54)$$

5.4. Influence of forming on damping-behavior of three layer sandwich sheet

As seen in chapter 0 the bending stiffness B_i for a sheet layer is significant for decay-behavior. With increasing stiffness of the cover layers, the total loss factor of the sandwich sheet decreases. Accordingly, the forming geometry has a big influence on the damping behavior. Cover-sheets with a thickness of $d_1 = d_2 = 1\,mm$ and a width and length with $b = l = 30\,mm$ and the viscoelastic interlayer (calculated adhesive, Figure 15) are shown in Figure 19. No. 1 shows the decay curve of an unformed sheet in contrast to a sheet with bended edges and a v-profile. All three sheets have the same initial width b. A great influence of the bending stiffness can be seen.

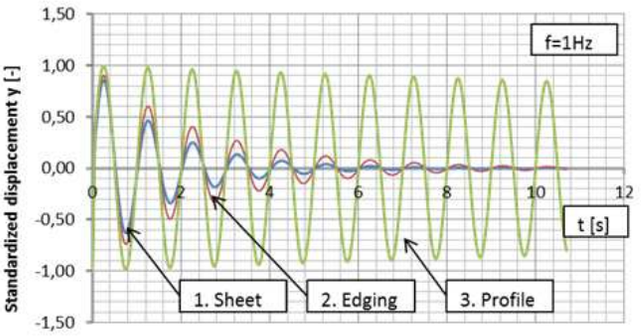

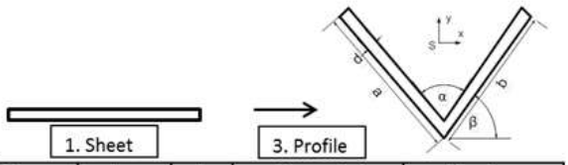

Geometry	tan $\delta_{sandwich}$ [-]	δ [1/s]	Moment of inertia I_{gesamt} [mm⁴]	Bending stiffness B'_{gesamt} [Nmm]
1	0,19	0,61	2,5	1566465,87
2	0,13	0,40	7,2	2697895,142
3	0,01	0,02	220	58946508,89

Figure 16. Damping effect of a three layer sandwich sheet, for an unformed, standardized displacement

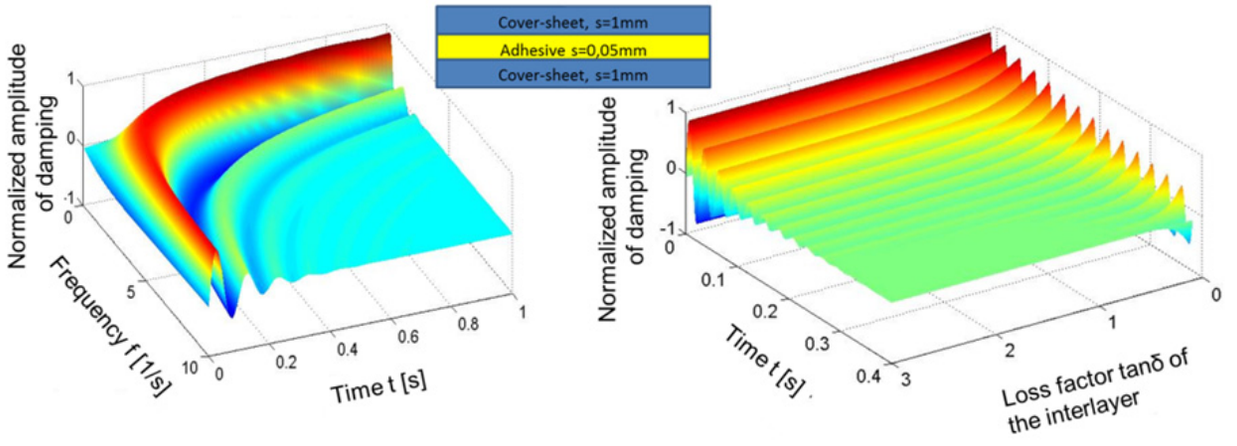

Figure 17. Influence of frequency and loss factor tanδ for a three layer sandwich-sheet

In Figure 17 the decay curve for different frequencies is shown. The loss factor tan δ of the adhesive is the main parameter of damping for a three layer sandwich-sheet. This factor is varied from zero to 3. A loss factor of tan δ = 2 is used for further investigations.

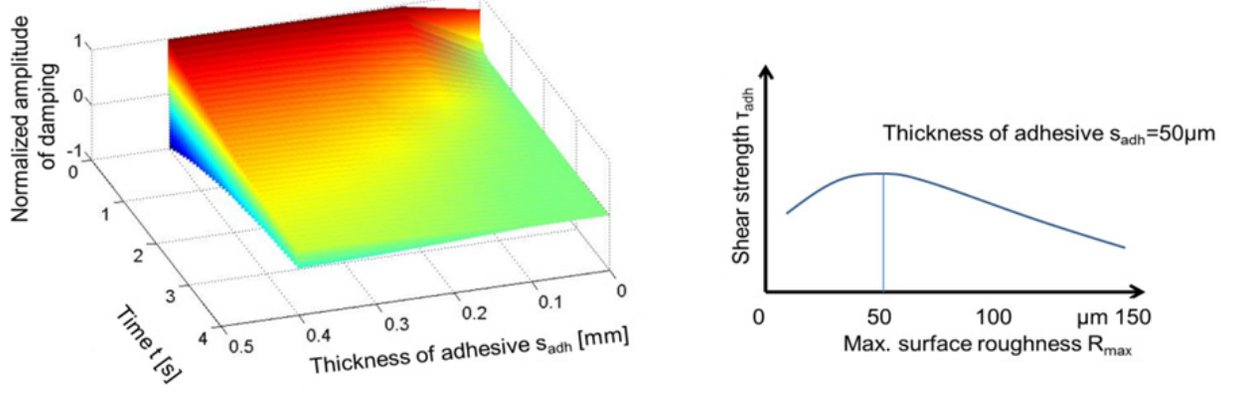

Figure 18. Influence of adhesive-thickness on damping behavior; and shear strength [8]

With smaller thicknesses of the adhesives, better damping behavior can be achieved. For a zero thickness, the adhesive transmits no bending waves. In Figure 18 the relationship

between adhesive thickness, surface roughness R_{max} and bond strength is shown according to [8]. It is recommended that the adhesive thickness is equal to the surface roughness R_{max}. A smaller thickness avoids a complete coating. To achieve improvements in damping behavior the surface roughness and the thickness of the adhesive layer has to be reduced.

6. Optimization of vibration damping sandwich sheets

6.1. Comparison of numerical and plastomechanical calculations

Numerical die-bending results of side length L = 40 mm are shown in Figure 10. Now, the strain distribution of the upper and lower fiber of both layers are shown and compared with the plastomechanical preliminary design. Computation according to [25] offer a k-factor of $k_{i/o} = \pm 1$, which fits quite good for the maximum strain, calculated with a numerical method in the midst of the bending. The real positions of the neutral axis are shown schematically.

Inaccuracies of preliminary design are ascribed to the [25]:

- Constant thickness during and after the bending process
- Negligence of elastic behavior of the cover sheets
- Linearization of the material properties
- Linearization of the elongation distribution
- Constant strain over bending angle

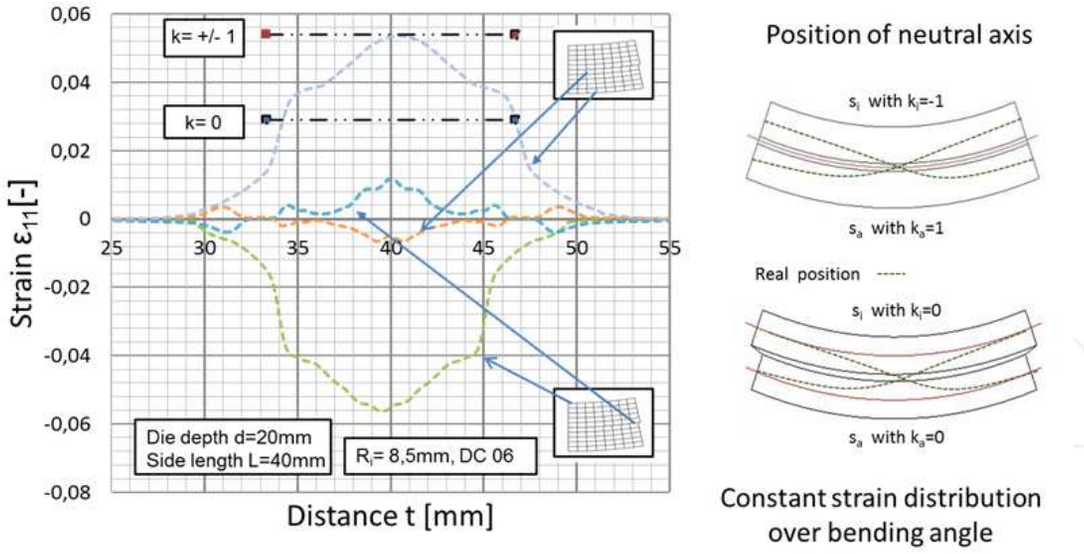

Figure 19. Numerical results of elongations of the external fibers (bending axis at distance t = 40 mm)

6.2. Forming tendencies of multilayer sandwich sheets

Thee founded results to influence the forming behavior, are further tested with simulation of v-die-bending. With a punch radius of r = 8,5 mm, a side length of L = 40 mm and a constant thickness of the sandwich s = 1,4 mm, the five typical constellations for different

layer thicknesses (Figure 20) are calculated. The same material as in chapter 3 and 6.1 is used. For this calculation, the adhesive thickness is neglected.

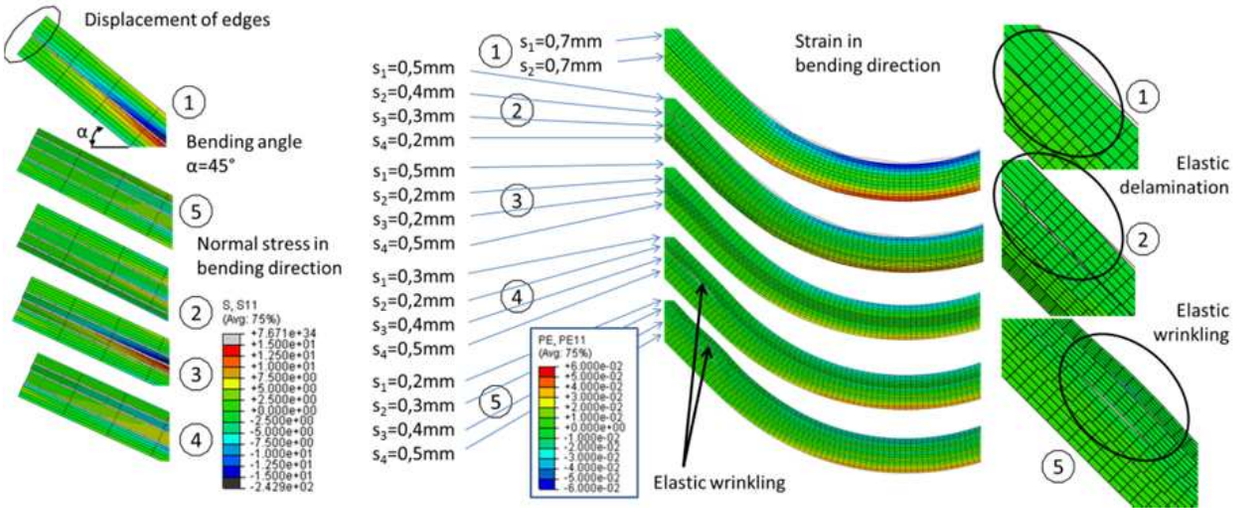

Figure 20. Numerical results of die-bending for five multilayer sandwich sheet

For this great side length, the displacement after forming is very small and no failure mode occurs for all five constellations. The symmetrical sandwich ($s_1 = s_2 = 0{,}7\ mm$) sheet no. 1 shows less spring back than all of the other constellations with 4 metal layers. The highest value for spring back shows no. 4 with increasing layer thickness. The remaining stress which can cause failure (chapter 1.2) decreases by using unsymmetrical thicknesses (no. 2, 3 and 4). As proposed in chapter 4.2, the number of layers influences the strain distribution. Minimal elongation shows specimen no. 3 and compression no. 5. Because of the minor stiffness no. 5 tends to buckling. This is an initial point for inner failures. The different spring back of each layer can be absorbed by the adhesive.

The normal plastic strain component in bending direction depends on the thickness of the metal layers. The thinner the inner cover sheet is, the minor is the plastic strain and the displacement of the edges (see no. 2-4). But a thin inner layer tends to buckling. To get the lowest normal stress in bending direction, the thickness should be increased as seen in configuration no. 4. Also the spring-back of the undamaged sandwich depends on the layer-configuration.

An example for an application of a commercial three-layer sandwich sheet in the automotive industry is shown in [25]. For this profile, formed by rolling the failures displacement, delamination and buckling could be predicted and verified with experimental tests.

7. Conclusions and forecast

At the Chair of Forming Technologies at the University of Siegen vibrations damping composite sheets were investigated regarding their forming limits.

During forming, failure modes like delamination, displacement and buckling of the cover sheets occur. The mechanical properties of the metal layers are determined by uniaxial

tensile tests. Tensile shear tests are carried out under variation of the shear velocity. The numerical calculations are calibrated with the tensile shear test. To verify the adhesive description, maximal tension and displacement in normal direction will be proved.

A plastomechanical preliminary design has been developed for sandwich sheets with a viscoelastic and shear transmitting interlayer. Especially displacement and delamination are described with preliminary design and verified with numerical calculations. But this plastomechanical preliminary design shows improvable deliverables. Especially the inaccuracies of the strain distribution over thickness and bending angle should be improved. Therefore many experimental forming tests with different materials are planned.

Instead of symmetrical sandwiches, significant improvements can be achieved by e.g. reducing the thickness of the outer metal layer. With increasing the number of sheets the total thickness of the composite can be achieved. On the other hand thin inner layers tend to buckling. The buckling tendency should be investigated further.

Author details

Bernd Engel and Johannes Buhl*
University of Siegen, Chair of Forming Technology, Siegen, Germany

Acknowledgement

A part of this present Investigation has been financially supported of Bundesministerium für Wirtschaft und Technologie (BMWi).

8. References

[1] Roos E, Maile K. Werkstoffkunde für Ingenieure Berlin Heidelberg: Springer; 2005.
[2] Lange K. Umformtechnik: Blechbearbeitung, Handbuch für die Industrie und Wissenschaft Berlin Heidelberg: Springer-Verlag; 1990.
[3] Jandel B, Meuthen AS. Coil Coating Wiesbaden: Vieweg & Sohn Verlag; 2008.
[4] Antiphon. antiphon® MPMTM - vibration damping sandwich material. [Online].; 2010 [cited 2010 04 21. Available from: www.antiphon.se.
[5] ThyssenKrupp Steel. Bondal® Körperschalldämpfender Verbundwerkstoff. [Online].; 2009 [cited 2010 04 21. Available from: www.thyssenkrupp-steel.com.
[6] Engel B, Buhl J. Metal Forming of Vibration-Damping Composite Sheets. steel research international. 2011;(DOI: 10.1002/srin.201000205).
[7] Hellinger V. New Possibilities for Improved Bending of Vibration Damping Laminated Sheets. CIRP annals: manufacturing technology. 1999.
[8] Habenicht G. Kleben Heidelberg: Springer-Verlag; 2009.

* Corresponding Author

[9] Keßler L. Simulation der Umformung organisch beschichteter Feinbleche und Verbundwerkstoffe mit der FEM Aachen: Shaker; 1997.
[10] Palkowski H, Sokolova O, Carrado A. Reinforced matel/polymer/metal sandwich composite with improved properties. In The Minerals M&MS. TMS 2011, 140th Annual Meeting & Exhibition. New Jersey: Joh Wiley & Sons, Inc., Hoboken; 2011.
[11] Sirichai T. Modellierung und Simulation eines Verbunds von Sandwichplatten zur Entwicklung einer mechanischen Verbindungstechnik RWTH Aachen: Doctoral thesis; 2007.
[12] Pickhan U. Untersuchungen zum abrasiven Verschleißverhalten, Biegeumformen und Verbindungsschweißen walz- und schweißplattierter Grobbleche Siegen: Höpner u. Göttert; 1998.
[13] Yanagimoto J, Oya a T, Kawanishi a S, Tiesler N, Koseki T. Enhancement of bending formability of brittle sheet metal in multilayer metallic sheets. CIRP Annals - Manufacturing Technology 59. 2010: p. 287–290.
[14] Ohashi Y, Wolfenstine J, Koch R, Sherby O. Fracture Behavior of a Laminated Steel–Brass Composite in Bed Tests. Materials Science and Engineering. 1992.
[15] Köhler M. Plattiertes Stahlblech Düsseldorf: Stahl-Informations-Zentrum; 2006.
[16] Deutsches Institut für Normung. DIN 50125 Prüfung metallischer Werkstoffe - Zugproben. In. Berlin: Beuth Verlag GmbH; 2004.
[17] Swift HW. Plastic Instability under Plane Stress. Journal of the Mechanics and Physics of Solids 1, Department of Engineering, University of Sheffield UK. 1952: p. 1–18.
[18] Groche P, von Breitenbach G, Steinheimer R. Properties of Tubular Semi-finished Products for Hydroforming. steel research international 76, No. 2/3, Stahleisen GmbH, Düsseldorf. 2005.
[19] Normenausschuss Materialprüfung (NMP), Materials Testing Standards Committee. Prüfung von Klebverbindungen- Probenherstellung Berlin: Beuth Verlag GmbH; 2006.
[20] Normenausschuss Materialprüfung (NMP) MTSC. Strukturklebstoffe - Bestimmung des Scherverhaltens struktureller Klebungen - Teil 2: Scherprüfung für dicke Fügeteile (ISO 11003-2:2001, modifiziert); Deutsche Fassung EN 14869-2:201 Berlin: Beuth Verlag GmbH; 2011.
[21] Nutzmann M. Umformung von Mehrschichtverbundblechen für Leichtbauteile im Fahrzeugbau Aachen: Shaker Verlag; 2008.
[22] Alfano G, Crisfield MA. Finite element interface models for the delamination analysis of laminated composites: mechanical and computational issues. International Journal for Numerical Methods in Engineering. 2001.
[23] Hashimoto K, Ohwue T, Takita M. Formability of steel-plastic laminated sheets. In Group 1bcotIDDR. Controlling sheet metal forming processes. Metals Park, Ohio: ASM International; 1988.
[24] Takiguchi M, Yoshida F. Effect of Forming Speed on Plastic Bending of Adhesively Bonded Sheet Metals. JSME International Journal Series A. 2004.
[25] Engel B, Buhl J. Roll Forming of Vibration-Damping Composite Sheets. In The 8th international Conference and Workshop on numerical simulation of 3d sheet metal forming processes.: AIP Conference Proceedings, Volume 1383, pp. 733-741; 2011.

[26] Banks J. AutoSimulations, Inc., Atlanta, GA 30067, U.S.A. Introduction to simulation. In P. A. Farrington HBNDTSaGWEe. Proceedings of the 1999 Winter Simulation Conference. Atlanta,: Print ISBN: 0-7803-5780-9; 1999.
[27] M. Weiss, B. F. Rolfe, M. Dingle, J. L. Duncan. Elastic Bending of Steel-Polymer-Steel (SPS) Laminates to a Constant Curvature. Journal of Applied MechANICS. 2006.
[28] Takiguchi M, Yoshida F. Deformation Characteristics and Delamination Strength of Adhesively Bonded Aluminium Alloy Sheet under Plastic Bending. JSME International Journal. 2003.
[29] Hudayari Ġ. Theoretische und experimentelle Untersuchungen zum Walzrunden von plattierten und nicht-plattierten Grobblechen Siegen : Höpner und Göttert; 2001.
[30] Fritzen CP. Technische Mechanik II (Elastomechanik) Siegen: UNI SIEGEN; 2006.
[31] Kreulitsch, H. Voest-Alpine Stahl Linz GmbH. Formgebung von Blechen und Bändern durch Biegen Wien: Springer; 1995.
[32] Lerch R, Sessler G, Wolf D. Technische Akustik: Grundlagen Und Anwendungen Heidelberg: Springer; 2008.
[33] Möser M, Heckl M, Kropp W, Cremer L. Körperschall: Physikalische Grundlagen und Technische Anwendung Heidelberg: Springer; 2010.
[34] Pflüger M, Brandl F, Bernhard U, Feitzelmayer K. Fahrzeugakustik Wien New York: Springer; 2010.
[35] Knaebel M, Jäger H, Mastel R. Technische Schwingungslehre Wiesbaden: Vieweg+Teubner | GWV Fachverlage GmbH; 2009.
[36] Ross D, Ungar E, Kerwin E.. Damping of Flexural Vibrations by Means of Viscoelastic Laminate. Structural Damping. 1959.
[37] Mead DJ, Markus S. The forced vibration of a three-layer, damped sandwich beam with arbitrary boundary conditions. Journal of Sound and Vibration. 1969.
[38] Sadasiva Rao YVK, Nakra BC. Vibrations of Unsymmetrical Sandwich Beams and Plates With Viscoelastic Cores. Journal Sound Vibrations. 1974.
[39] Mead DJ. A comparison of some equations for the flexural vibration of damped sandwich beams. Journal Sound Vibration. 1982.
[40] Dewangan P. Passive viscoelastic conatrained layer damping for structural application. National Institude of Technology Rourkela. 2009.